J. Biomed. Eng. Res : 471-476, 2007

Development of Effective Analytical Signal Models for Functional Microwave Imaging

Sungkeun Baang, Jong Dae Kim, Yong-Up Lee, Chan Young Park

Division of Information Engineering and Telecommunications, Hallym University
(Received May 23, 2007. Accepted June 29, 2007)

Abstract

Various active microwave imaging techniques have been developed for cancer detection for past several decades. Both the microwave tomography and the UWB radar techniques, constituting functional microwave imaging systems, use the electrical property contrast between normal tissues and malignancies to detect the latter in an early development stage. Even though promising simulation results have been reported, the understanding of the functional microwave imaging diagnostics has been relied heavily on the complicated numerical results. We present a computationally efficient and physically instructive analytical electromagnetic wave channel models developed for functional microwave imaging system in order to detect especially the breast tumors as early as possible. The channel model covers the propagation factors that have been examined in the previous 2-D models, such as the radial spreading, path loss, partial reflection and transmission of the backscattered electromagnetic waves from the tumor cell. The effects of the system noise and the noise from the inhomogeneity of the tissue to the reconstruction algorithm are modeled as well. The characteristics of the reconstructed images of the tumor using the proposed model are compared with those from the confocal microwave imaging.

Key words : microwave imaging, signal modeling, noise, breast cancer, tumor

I. INTRODUCTION

There has been significant progress toward the non-ionizing imaging of the human body to detect the cancers using electromagnetic waves. The microwave imaging represents such effort to detect cancers at early stage. Among three types of application of microwave, passive, active and hybrid, the active microwave imaging has also three proposed techniques: micowave tomograhy, ultrawide-band microwave radar techniques and hybrid imaging. Functional microwave imaging for breast tumor detection uses the electrical property contrast between normal tissues and malignancies of breast tissues as shown in Figure 1. Normal breast tissues is more translucent to microwaves and the ratio of electric properties of malignant to normal breast tissue is more than factor of 3 or so.

This work was supported by the Korea Research Foundation Grant funded by the Korean Government (MOEHRD) (KRF-2006-331-E00250).
Corresponding Author : Sungkeun Baang
Division of Information Engineering and Telecommunications, Hallym University, 1 Okchon-dong, Chunchon, Gangwon-do, 200-702 Korea
Tel : 033-248-2349 / Fax : 033-242-2524
E-mail : baang@hallym.ac.kr

To the comparison, the mammogram, X-ray imaging of a compressed breast is based on the variation of tissue density. It is reportedly to miss up to 15 % of breast cancers. And, less than 10 % of the suspicious areas by the mammogram were diagnosed as malignancies [3]. Microwave imaging diagnostic has known advantages to the mamogram such as low health risk, cost effective, acceptably comfortable, objective and consistent results as well as nonivasiveness and sensitivity.

Active microwave imaging uses short electromagnetic pulse and synthetically focuses backscattered signals to create images that indicate regions of significant scattering. Recent numerical studies show that spatial resolution of microwave imaging can be obtained in the scale of a few millimeter. However, reported works with microwave imaging use 2-D or more complicated models of the breast and electromagnetic wave propagation and heavily rely on the numerical simulation results using such a finite-difference-time-domain (FDTD) method.

It would be very helpful if the signal of microwave imaging can be approximated into a convenient analytical equation, since, then, it provides us the room to apply the well-known techniques of physics and engineering to the microwave imaging signals. The breast tissue model used in the confocal microwave imaging by Fear and others [1-5] assumed discrete tissue parameters and solved the reflection deterministically.

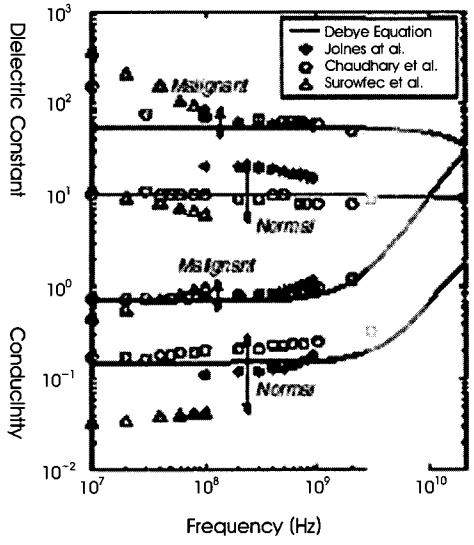

Fig. 1. Electric properties of normal and malignant breast tissue at radio and microwave frequencies : dielectric constants and condutivities (Ref. [6]).

However, the uncertainties in measurement and reflection can be detrimental to the reconstruction of the image. It is necessary to evaluate the probabilistic nature of microwave imaging signals using appropriate noise models.

Therefore, we propose the analytical expression of microwave imaging signals that is effective for calculation and provides us more physical insight than the numerical simulations. The effectiveness of the approximate expression can be examined by the comparison of the reconstructed images using the presented model and those from the previous numerical simulations. The effects of system noise are considered using a Gaussian noise model and the inhomogeneous tissure effects to the signal characteristics are addressed using a random scatterer model.

II. MICROWAVE IMAGING SIGNAL MODELS

A. Microwave Signal Model

Since the dielectric constants of the breast tissues show a fairly flat distribution over a range of frequency of interest, we assume that dispersion effects can be neglected in the microwave imaging. And we also assume that the reflections from the skin and tumors are significant, and that the incident wave travels through skin, tissue, tumors and backscatters to the antennas keeping the incident waveform. The permeability of the human tissues is assumed to be that of free-space one.

When traveling the tissue which has the characteristic properties of $(\epsilon,\ \sigma,\ \mu_0)$, the complex propagation constant of EM wave can be expressed as:

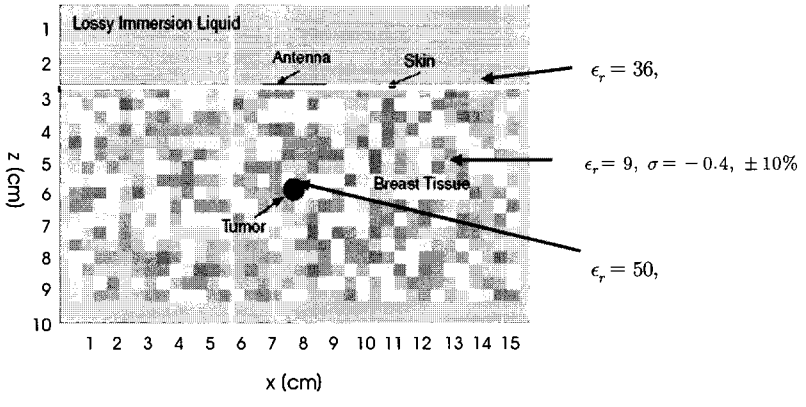

Fig. 2. Planar model of breast tissues bearing a tumor (Ref. [1]).

$$\gamma = \alpha + j\beta$$

where α and β are attenuation coefficient and wave number of the EM wave, and ϵ, σ and μ_0 are the electric permittivity, the electric conductivity and the permeability of free space, respectively.

In the planar model, we use the same parameters as in the previous works as in Figure 2 [1].

In order to focus the breast synthetically, the EM wave velocities in each region of the tissues need to be determined. The traveling velocity of the EM wave can be obtained approximately as [7]

$$v = \frac{\omega}{\beta} \approx \frac{c}{\sqrt{\epsilon_r}} \tag{1}$$

Then, in each region of tissue, the normalized velocities by the free-space light speed c can be written as listed in Table I.

The return times of the reflected signals by the proposed tissue model are calculated using the tissue velocities in Table I. They are compared to those from the previous model. From this observations, it is found that the traveling velocity of EM wave can be approximated as V_t. The comparison results of the return times of the reflected signals are summarized in Table II.

In order to evaluate the reflected power properly, the attenuation of the EM wave is taken into account. We assume that the attenuation is due primarily to the radial spreading, the path loss and the partial reflection and transmission. The radial spreading assumes r^{-2} variation of power using the spherical wave approximation. Since the reflected signal can be thought as originated from the tumor, the reflected voltage takes the r^{-2} variation when r is the single path distance. The path loss is accounted by the loss coefficient of the complex phase constant. Therefore, the reflected voltage from the tumor can be expressed as

$$V_{tumor}(t) = A(r)\, V_0(t - t_{tumor}) \tag{2}$$

where the amplitude coefficient $A(r)$ is given by

$$A(r) = K\frac{1}{r^2}e^{-2ar} \tag{3}$$

$$\alpha \approx \frac{\sigma}{2}\sqrt{\frac{\mu}{\epsilon'}} = \frac{\sigma}{2}\frac{\eta_0}{\sqrt{\epsilon_r}} \quad \text{(loss coefficient)}, \tag{4}$$

and η_0, ϵ_r are the intrinsic impedance of free space and the relative permittivity, respectively.

Here, the constant K is determined from the various aspects such as tumor reflection coefficient and antenna alignment. In order to avoid the complex near field effects of the antenna, we assume that r is large enough compared to the skin depth of the center frequency of the EM wave:

$$r > \delta_s$$

where the skin depth of the skin δ_s is

$$\delta_s = 1/\sqrt{\pi f_0 \mu\sigma} \sim 1cm$$

The loss coefficients and the path losses in each of the breast tissues are summarized in Table III.

As can be seen in Table III, the path loss in the normal tissue is the least significant one (2.2 dB/cm). And this value is closely consistent with the results of the FDTD simulation of 2 ~3 dB/cm [1].

In reference [1], the ratio of the peak-to-peak tumor response to the excited voltage, from a 6 mm diameter tumor located 3 cm below the skin is found to be -94.1 dB. From the finding, we can determine the constant K as

Table 1. The traveling velocities in the breast tissue model.

	Skin (V_s)	Tissue (V_t)	Tumor(V_m)
normalized velocity	0.16	0.33	0.14

Table 2. *The return times calculated and determined from the simulation results [1].*

	Skin	Tumor Upper Edge	Within Tumor
Thickness	2mm	3cm	6mm
Return time by (1)	0.08ns	0.686ns	0.12ns
Return time by [1]	–	0.698ns	0.16ns

Table 3. The loss coefficients and the loss ratios.

	Skin	Tissue	Tumor
α (Np/m)	125.6	25.1	106.6
Loss ratio (%/cm)	28.5 (10.9 dB/cm) (78%/2mm)	77.8 (2.2 dB/cm)	34.4 (9.3 dB/cm)

$$y = 20\log\left(1/Kr^{-2}e^{-2ar}\right) \text{ attenuation} \tag{5}$$

$$K = r^2 e^{2ar} e^{-\frac{y\ln 10}{20}} = 7.98\times 10^{-8} \tag{6}$$

Then, the response from the tumor by the microwave imaging assumes the following form:

$$V_R(t) = V_0(t) + V_u(t) + V_l(t) = V(t) + A(r_u)V(t-t_u) + A(r_l)V(t-t_l) \tag{7}$$

where

$V_R(t)$ the total signal at the antenna,

$V_0(t)$ the incident (excited) signal voltage,

$V_u(t-t_u)$ the reflected voltage from the upper edge of the tumor,

$V_l(t-t_l)$ the reflected voltage from the lower edge of the tumor,

$A(r)$ the attenuation coefficient,

$$A(r) = \begin{cases} Kr^{-2}e^{-2ar} & r > 1cm \\ 1 & r \le 1cm \end{cases} \tag{8}$$

t_u, t_l the time required to travel from the antenna to the upper and lower edges of the tumor and back to the antenna, respectively,

$$t_u = \frac{2r_u}{v_t} + t_s \quad t_l = \frac{2r_l}{v_t} + t_s = t_u + \frac{2d_{tumor}}{v_t} \tag{9}$$

t_s the time required to travel from the antenna to the skin and back to the antenna,

d_{tumor} the tumor diameter,

r_u, r_l the distance from the antenna to the upper and lower edges of the tumor, respectively.

Here, the reflection from the skin and the excitation signals will be eliminated through the calibration.

B. Noise Models

We first generate noise-free signal from the above signal model with a differentiated Gaussian pulse excitation of peak voltage of 1. Then, noise effects can be investigated afterwards, by adding appropriate noise signals to the reflected signals. Synthetic focusing is applied to the processed data and the effects of Gaussian noise are investigated. The noise power of the Gaussian noise is normalized by the incident signal power.

Inhomogeneous variation of the dielectric constants over the tissues will result as unwanted signals of random amplitude. It is reasonable for the random reflections to occur in random positions, as long as there is no generic breast tissue model applicable to all of the patients. Based on the reasoning, the noisy reflections can be integrated into the model with random point-scatterers that have random positions and reflection constants. Their existences were determined by thresholding a uniform random variable. Therefore their occupancy rate of a unit space is equal to the threshold P. The relative reflection constants were assumed to be uniformly distributed. Then, the final reflection constant was multiplied by a mean reflection constant R_o.

Each of the scatterer noise can be characterized by its reflection coefficient and position: $s_i = (R_i, x_i)$ assuming R_i and x_i are distributed independently. Then an antenna signal is corrupted by noise with the form of the following equation;

$$n_s(t) = \sum_i A(r(s_i))R_i V(t-t_i) \tag{10}$$

where R_i, r_i, and t_i are the reflection constant distance, the position and the arrival time from i-th random scatterer, respectively.

III. IMAGE RECONSTRUCTION RESULTS

In order to compare the results with those of the previous simulation works, we assume the same configuration as in [1]. In the planar configuration, shown in Figure 3, the antenna spans 6 cm, skin thickness 2 mm, and the tumor location about

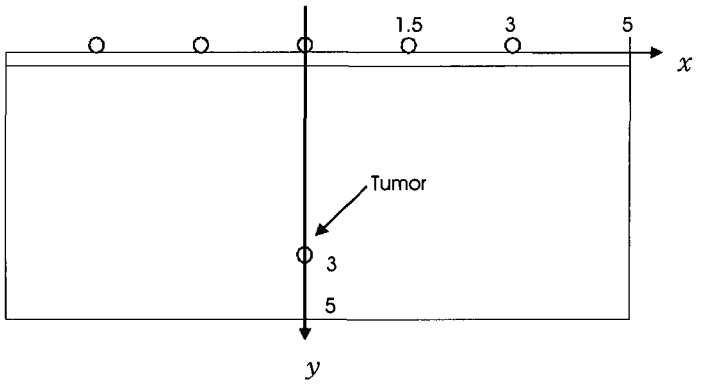

Fig. 3. Planar configuration: Antenna position = {(-3,0),(-1.5,0),(0,0),(1.5,0),(3,0)}, Tumor radius = 0.3, Skin thickness=0.2, Tumor center = (0,3.5).

3.5 cm below the skin. We take the imaging area as a 10 cm x 5 cm rectangle below the antennas with the resolution of 1 mm, which corresponds to the time resolution of 0.01 ns. With the use of tissue velocity, the maximum delay is about 1.2 ns. We take the signal during 5 ns with the time resolution of 0.001 ns resulting 5000 x 5 double precision data.

We first generate noise-free signal from the above signal model with a differentiated Gaussian pulse excitation of peak voltage of 1. Then, noise effects can be investigated afterwards, by adding appropriate noise signals to the reflected signals. Thus, each pixel in the imaging area in Figure 3 has the coordinates as follows:

$$x_i = 1mm * i - 5cm \qquad i = 0,1,\cdots,1000$$
$$y_j = 1mm * j \qquad j = 0,1,\cdots,500$$

Using the coordinates given above, we can get the microwave images by the same reconstruction scheme explained in ref [3]. A brief summary of the scheme is presented, here:

A. Calibration: The calibration process eliminates the unwanted reflection from the skin. The signal of the l-th antenna is subtracted by the average of signal from each signal.

$$[V_C(k)]_l = [V_R(k)]_l - \sum_{l=1}^{N} \frac{[V_R(k)]_l}{N} \quad l = 1,\cdots,N \tag{11}$$

where k is the time index, l the index of the antenna, and N the total number of the antennas.

B. Integration: Transforms the center of signal from zero to maximum.

$$[V_l(m)]_l = \sum_{k=1}^{m} [V_c(k)]_l \tag{12}$$

where m is the newly assigned time index.

C. Compensation: Account the round-trip attenuation from the source.

$$[V_G(m)]_l = [V_I(m)]_l * G(m) \tag{13}$$

$$G(m) = \begin{cases} \frac{1}{k} r_{tissue}^2 e^{2ar_{tissue}} & r_{tissue} > 1cm \\ 1 & r_{tissue} \le 1cm \end{cases} \tag{14}$$

$$r_{tissue} = t_{tissue} \cdot V_t \tag{15}$$

$$t_{tissue} = t - t_s - t_0 = \frac{m}{1000} - t_s - t_0 \text{ (ns)} \tag{16}$$

where t_0 is the excitation time.

D. Image reconstruction: Scan focal point through the breast tissues to create image. The intensity at the pixel position $r = (x_i, y_j)$ is given by

$$I(r) = \left(\sum_{i=1}^{N} [V_G(\tau_l(r)]_l \right)^2 \tag{17}$$

where $[V_G(\tau_l(r)]_l$ is the post-processed backscatter waveform at the l-th antenna located at r_l and $\tau_l(r)$ the discrete time delay from the l-th antenna to the synthetic focal point at r.

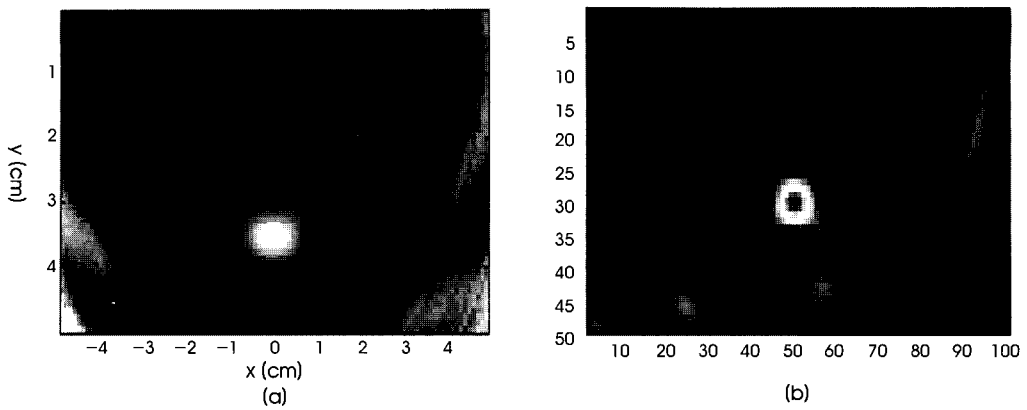

Fig. 4. (a) The reconstructed image of the tumor-bearing tissues using Gaussian noise model with a normalized noise power of 5e-3, (b) The reconstructed image of the tumor-bearing tissues with point-scatter noise model.

$$\tau_l(r) = \frac{2|r - r_l|}{V_t \, \Delta t} \tag{18}$$

The reconstructed images in Figure 4 show similar reflection patterns and tumor dimensions as in previous works. However, as expected, Figure 4 also shows that the reconstructed images get deteriorated as the noise level increases.

IV. DISCUSSION

This paper presents an efficient and physically instructive electromagnetic wave channel modeling for microwave imaging system especially for the breast tumor detection. The proposed model takes account the radial spreading, path loss, partial reflection and transmission of the backscattered electromagnetic wave from the tumor cell. Then, the effects of two kinds of noise sources to the reconstruction algorithm were investigated employing the gaussian noise model for the system noise and the random point-scatterer model for the inhomogeneous tissue.

Synthetic focusing is applied to the processed data and the effects of the noise are investigated. The resulting breast images are shown in Figure 4(a). The noise power of the Gaussian noise is normalized by the incident signal power. It is shown that the noise signals generated from far away from the antenna give rise to a significant effect to the image reconstruction. Therefore, the amplitude compensation needs to be carefully applied when accounting the noise effects.

Fig. 4(b) shows an example image corrupted by random point-scatterer noise. The lattice distance and the occupancy probability were set to 4 mm and 1, respectively. And the mean reflectance were selected as 1/1000 of the maximum of the antenna signals. The image with point-scatterer noise model takes after more the FDTD simulation results.

The reconstructed images in this paper are generated by 41 coplanar antennas signals and they show similar reflection patterns and tumor dimensions as in previous works. This promises that confocal microwave imaging can be modeled realistically despite of the simplicity and the intuitivity of the presented methods.

REFERENCES

[1] E. C. Fear, X. Li, S. C. Hagness, and M. A. Stuchly, "Confocal microwave imaging for breast cancer detection: localization of tumors in three dimensions," *IEEE Trans. Biomed. Eng.*, vol. 49, pp. 812-821, Aug. 2002.

[2] S. C. Hagness, A. Taflove, and J. E. Bridges, "Three-dimensional FDTD analysis of a pulsed microwave confocal system for breast cancer detection: design of an antenna-array element," *IEEE Trans. Antennas Propagat.*, vol. 47, pp. 783-791, May 1999.

[3] E. C. Fear, S. C. Hagness, P. M. Meaney, M. Okoniewski, and M. A. Stuchly, "Enhancing breast tumor detection with near-field imaging," *IEEE Microwave Magazine,* pp. 48-56, Mar. 2002.

[4] S. C. Hagness, A. Taflove, and J. E. Bridges, "FDTD analysis of a pulsed microwave confocal system for breast cancer detection," in *Proc. 19th Int. Conf. IEEE/EMBS*, Chicago, IL. USA, Oct. 30 - Nov. 2, 1997, pp. 2506-2508 .

[5] S. C. Hagness, A. Taflove, and J. E. Bridges, "Two-dimensional FDTD analysis of a pulsed microwave confocal system for breast cancer detection: fixed focus and antenna-array sensors," *IEEE Trans. Biomed. Eng.*, vol. 45, pp. 1470-1479, Dec. 1998.

[6] X. Li and S. C. Hagness, "A confocal microwave imaging algorithm for breast cancer detection," *IEEE Microwave Wireless Components Lett.*, vol. 11, pp. 130-132, Mar. 2001.

[7] W. Hayt, Jr. and J. Buck, *Engineering Electromagnetics*, New York, McGraw-Hill, 2001, pp. 356-365.